

Scaling in long term data sets of geomagnetic indices and solar wind ϵ as seen by WIND spacecraft.

B. Hnat¹, S.C. Chapman¹, G. Rowlands¹, N.W. Watkins² and M.P. Freeman²

We study scaling in fluctuations of the geomagnetic indices (AE , AU , and AL) that provide a measure of magnetospheric activity and of the ϵ parameter which is a measure of the solar wind driver. Generalized structure function (GSF) analysis shows that fluctuations exhibit self-similar scaling up to about 1 hour for the AU index and about 2 hours for AL , AE and ϵ when the most extreme fluctuations over 10 standard deviations are excluded. The scaling exponents of the GSF are found to be similar for the three AE indices, and to differ significantly from that of ϵ . This is corroborated by direct comparison of their rescaled probability density functions.

1. Introduction

The statistical properties of fluctuations in geomagnetic indices and their relation to those in the solar wind, is a topic of considerable interest (see, e.g., [Sitnov *et al.*, 2000; Tsurutani *et al.*, 1990; Ukhorskiy *et al.*, 2002; Vörös *et al.*, 1998]). Scaling has been identified as a key property of magnetospheric energy release in the form of bursty bulk flows in the magnetotail [Angelopoulos *et al.*, 1992], “blobs” in the aurora [Lui *et al.*, 2000], non-Gaussian fluctuations in geomagnetic indices [Hnat *et al.*, 2002, 2003a; Consolini *et al.*, 1996] and in single station magnetometer data [Kovács *et al.*, 2001; Vörös *et al.*, 1998]. Models include Self-Organized Criticality (SOC) [Chang *et al.*, 2003] (see also the review [Chapman and Watkins, 2001]) and multi-fractal models [Kovács *et al.*, 2001] related to those of turbulence [Consolini *et al.*, 1996; Vörös *et al.*, 1998].

These measures of scaling and non-Gaussian fluctuations in magnetospheric output need to be understood in the context of the system’s driver, the solar wind, which is turbulent and thus also scaling. Other work has focussed on comparing properties of input parameters such as ϵ and the indices (AE , AU and AL) to establish whether they are directly related. However, these studies have not provided a consistent answer. While Freeman *et al.* [2000] found that both the ϵ and the AU and AL indices exhibited nearly identical scaling of burst lifetime probability density functions (PDFs), Uritsky *et al.* [2001] obtained quite different scalings for AE and the solar wind quantity $v_x B_{yz}$ using spreading exponent methods motivated by SOC. Hnat *et al.* [2002, 2003a] used a PDF rescaling technique to characterize the fluctuation PDF of 4 years

¹Space and Astrophysics Group, University of Warwick
Coventry, CV4 7AJ, UK

²British Antarctic Survey, Natural Environment Research
Council, Cambridge, CB3 0ET, UK

ϵ data from WIND and a 1 year data set of *AE* indices with fluctuations over a few standard deviations. Direct comparison of the PDF's functional form suggested close similarity to within statistical error.

In this paper we use a larger 10-year data set for the *AE* indices to obtain a more accurate statistical determination of the functional form of the PDF of fluctuations over a more extensive dynamic range, including characterization of extremal events up to 10 standard deviations for the first time. We apply structure functions to characterize and compare both the low and higher order moments for all quantities. A 4-year subset of the index data, corresponding to the same period in the solar cycle as that used to produce ϵ , is used to facilitate this comparison. We then verify these results by direct examination of the fluctuation PDF using the full 10-year *AE* indices dataset.

2. Data Sets

The *AL*, *AU* and *AE* index data sets investigated here comprise over 5.5 million, 1 minute averaged samples from January 1978 to December 1988 inclusive. The ϵ data set is identical to that used in *Hnat et al.* [2002, 2003a] and extends from January 1995 to December 1998 inclusive. It includes intervals of slow and fast speed streams. ϵ is defined (see [*Hnat et al.*, 2002]) in SI units as $\epsilon = v(B^2/\mu_0)l_0^2 \sin^4(\Theta/2)$, where $l_0 \approx 7R_E$ and $\Theta = \arctan(|B_y|/B_z)$, and was calculated from the WIND spacecraft key parameter database [*Lepping et al.*, 1995; *Ogilvie et al.*, 1995]. The indices and ϵ are from different time intervals and here we assume statistical stability over these long time intervals.

3. Generalized Structure Functions

Generalized structure functions (GSF), or generalized variograms, can be defined in terms of an average over time of a differenced variable $\delta x(t, \tau) = x(t + \tau) - x(t)$ as $S_m(\tau) = \langle |\delta x(t, \tau)|^m \rangle$ [*Rodríguez-Iturbe and Rinaldo*, 1997]. If δx exhibits scaling with respect to τ , then $S_m \propto \tau^{\zeta(m)}$. A log-log plot of S_m versus τ should then reveal a straight line for each m with gradients $\zeta(m)$. If $\zeta(m) = \alpha m$ (α constant) then the time series is self-similar with single scaling exponent α .

In order to compare the scaling properties of the non-contemporaneous ϵ and *AE* indices time series, we select a 4-year subinterval 1984 – 1987 from the *AE* indices at the same phase in the solar cycle as the ϵ data. Figure 1 shows the second order GSFs as measured by the standard deviations $\sigma(\tau) = [S_2(\tau)]^{1/2}$ of the fluctuation $\delta x(t, \tau)$. A scaling region is apparent between 2^7 and 2^{12} s where $\sigma(\tau) \propto \tau^H$, where H is the Hurst exponent [$\zeta(2)/2$]. The R^2 goodness of fit analysis was performed to select the optimal power law region and gradient and results are summarized in Table 1. The upper limits of the scale regions τ_{max} are in good agreement with values reported previously [*Consolini and De Michelis*, 1998; *Takalo et al.*, 1993; *Takalo and Timonen*, 1998].

Any such single estimate of the H , whilst establishing the region of τ over which there is scaling, does not fully characterize the properties of the time series. For example, a fractional Brownian motion (fBm) can be constructed to share the same H value as *AE*, but the fBm series has Gaussian distributed increments δx by definition [*Mandelbrot*, 2002] whereas those of *AE* are non-Gaussian [*Consolini and De Michelis*, 1998; *Hnat et al.*,

2002]. As discussed by *Mandelbrot* [2002] the similar values arise because H aggregates *two* sources of scaling in monofractal random walks: persistence (the “Joseph” effect) and heavy tails in the increments (the “Noah” effect). In the above example the anomalous value of H for fBm comes just from the Joseph effect, whilst for AE the Noah effect must be at work. Furthermore, estimating H by only one method may not distinguish a fractal time series from a discontinuous one [*Watkins et al.*, 2001; *Katsev and L’Heureux*, 2003]. We thus turn next to the higher order m values of $\zeta(m)$.

Figure 2 shows scaling exponents $\zeta(m)$ derived from raw GSFs with m varying between -1 and 8 for the $\delta\epsilon$ and AE indices fluctuations. These suggest the departure of higher orders from self-similarity, i.e., $\zeta(m)$ departs from a straight line. The inset of this figure shows the origin of these $\zeta(m)$ values for δAU and $m = 1, \dots, 7$. Only the first four orders exhibit clear linear behavior expected in the scaling region. For higher orders, the value of ζ very strongly depends on the assumed extent of the scaling region to which one fits a straight line. In principle, $\zeta(m)$ can be obtained for any m . However, errors do not contribute uniformly over m , for example, the largest fluctuations that affect large m , are statistically poorly resolved, whereas the smallest fluctuations ($\delta x \rightarrow 0$) are dominated by instrument thresholds. For the latter reason we will exclude $m = -1$ for $\delta\epsilon$ as $\delta\epsilon \rightarrow 0$ is not well determined through its definition.

Conditioned GSFs quantify the impact of intermittency on fluctuations of different sizes by imposing a threshold A on the event size [*Kovács et al.*, 2001]. Here, this threshold will be based on the standard deviation of the differenced time series for a given τ , $A(\tau) = 10\sigma(\tau)$. This procedure allows us to exclude rare extreme fluctuations with large statistical errors which, for large m , could lead to a spurious departure from self-similar behavior. Alternatively, conditioning with different thresholds estimates a maximum size for the fluctuations for which self-similarity is still valid.

Following conditioning, log-log plots of $S_m^c(\tau)$ show good correspondence with straight line fits, shown for δAU in the inset of figure 3. This power law dependence holds between times already obtained from the R^2 analysis performed for $\sigma(\tau)$. The main plot then shows $\zeta(m)$ obtained from the conditioned $S_m^c(\tau)$. All lines in the figure were fitted for moments between -1 (0 for ϵ) and 6 and then extended to the entire range of data. Scaling exponents obtained from this technique were unchanged for thresholds $A(\tau)$ between 6σ and 12σ .

Firstly, our analysis suggests that the statistics of the fluctuations for all four quantities are self-similar for times between 2 and ~ 100 minutes and fluctuations of size $\delta x \leq 10\sigma(\tau)$. Secondly, the scaling exponent α in $\zeta(m) = \alpha m$ that characterize this self-similar behavior, are identical within errors for fluctuations in the AE indices but different to that in ϵ at the 1σ level.

4. Rescaling of Fluctuation PDFs

Scaling of the GSFs can be related to scaling properties of the fluctuation PDFs [*Hnat et al.*, 2002, 2003a] using the generic, model-independent rescaling method (e.g. [*Mantegna and Stanley*, 1995; *Hnat et al.*, 2003b]) based on the rescaling of the PDFs $P(\delta x, \tau)$ of $\delta x(t, \tau)$ on different time scales τ . If a time series exhibits statistical self-similarity, a single argument representation of the PDF can be found that is given by $P(\delta x, \tau) = \tau^{-\alpha} P_s(\delta x \tau^{-\alpha})$,

where α is the rescaling exponent. We now express S_m using the fluctuations' PDF, $P(\delta x, \tau)$ as follows:

$$S_m(\tau) = \int_{-\infty}^{\infty} |\delta x|^m P(\delta x, \tau) d(\delta x). \quad (1)$$

Expressing the integral in (1) in terms of rescaled variables P_s and $\delta x_s = \delta x \tau^{-\alpha}$ shows that the scaling exponent $\zeta(m)$ is a linear function of m , $\zeta(m) = m\alpha$, for a statistically self-similar process, as suggested here by figure 3.

The exponent α is ideally obtained from the scaling of the peaks of the PDF $P(0, \tau)$. However, the finite accuracy of the measurement may discretize the amplitude leading to errors in the peak values. Table 1 gives all scaling exponents, obtained by different methods. These yield consistent values of α , to within the errors. We will use α from the scaling of $\sigma(\tau)$ versus τ . If the fluctuations are statistically self-similar, as suggested by our GSF analysis, then the unscaled PDFs $P(\delta x, \tau)$ should collapse onto a single curve $P_s(\delta x_s)$. We applied PDF rescaling to the fluctuation PDFs of all quantities and obtained satisfactory collapse of the curves within the scaling regions. The χ^2 test applied to all quantities revealed that, for the scaling regions given above, the collapsed curves lie within 5 – 7% error band.

Figure 4 shows the re-scaled fluctuation PDFs for the indices alone for $\tau \approx 15$ min. The δx variable has been normalized to the rescaled standard deviation $\sigma_s(\tau \approx 15 \text{ min.})$ of P_s in each case to facilitate this comparison. The inset of this figure shows the comparison for AU , AE and $-AL$ fluctuations and these PDFs are nearly identical. These results are consistent with conclusions of the GSF analysis at the 1σ level.

Figure 5 shows the normalized PDFs $P_s(\delta x_s)$ for $\delta x = \delta\epsilon$, δAE and $\tau \approx 15$ min overlaid on a single plot. We can clearly distinguish between the PDFs of the $\delta\epsilon$ and AE indices' fluctuations. We obtain the same result repeating this comparison for several values of τ , within the scaling range τ_{max} . We have also verified that the functional form of the PDF are insensitive to the solar cycle within errors. The use of a larger, 10 year data set for the indices has reduced statistical scatter and expanded the dynamic range of the considered fluctuations as compared to the analysis given in [Hnat et al., 2002, 2003a], and would lead us to draw the opposite conclusion, that on time scales less than ≈ 1 hour the AE index amplitude fluctuations are not driven linearly by those of the solar wind. We would also conclude that the difference seen at the 1σ level in the scaling of the ϵ and the indices is significant, even though they agree at the 2σ level [Freeman et al., 2000].

5. Summary

In this paper we have addressed an open question of the possible connection between the scaling properties of fluctuations in the solar wind driver and those observed in global measures of magnetospheric dynamics. We applied two statistical methods, generalized structure functions and PDF rescaling, to study the scaling of fluctuations in the ϵ parameter and the magnetospheric indices AU , AL and AE . We find that, statistically, fluctuations in all four quantities are approximately self-similar when their size is limited to $\sim 10\sigma$. This self-similarity extends to $\sim 1 - 1.5$ hours. The scaling exponents of the AE indices are close to each other and are appreciably different to

that of the ϵ parameter.

The fluctuation PDFs of the *AE* indices, unlike that of $\delta\epsilon$, are asymmetric. Direct comparison of the PDFs for the fluctuations in the *AU*, *AE* and $-AL$ index indicates that they are nearly identical. Whilst the low frequency behavior of the solar wind and the indices may be well correlated [Tsurutani *et al.*, 1990], here we have concluded that, on time scales smaller than 1 hour the properties of the fluctuations in the solar wind and the indices differ in *both* amplitude and persistence. If the underlying physical origin of the auroral scaling is turbulence, then different scaling behavior implies a different type of turbulence, i.e., different dimensionality/topology or different relevant physics [Frisch, 1995]. If the underlying physics is SOC or similar [Chang *et al.*, 2003] then similar conclusions would still be drawn (c.f. [Uritsky *et al.*, 2001]). However, at this point we also can not rule out the possibility that the way in which the indices are constructed “burns” information still present in the magnetometer data about the solar wind scaling, here possibly by changing either or both of the degree of persistence (power spectral slope) and the heavy-tailed property (see [Edwards *et al.*, 2001] for a related preliminary investigation).

6. Acknowledgment

SCC and BH acknowledge the PPARC and GR the Leverhulme Trust. We thank R. P. Lepping and K. Ogilvie for provision of data from the NASA WIND spacecraft and the World Data Center C2, Kyoto for geomagnetic indices.

References

- Angelopoulos, V. *et al.*, Bursty bulk flows in the inner central plasma sheet, *J. Geophys. Res.*, **59**, 4027–4039, 1992.
- Chang, T., S. W. Y Tam and C. C. Wu, Complexity induced anisotropic bimodal intermittent turbulence in space plasmas, *Phys. Plasmas*, in press, 2003.
- Chapman, S. C., and N. W. Watkins, Avalanching and Self-Organised Criticality: a paradigm for magnetospheric dynamics?, *Space Sci. Rev.*, **95**, 293–307, 2001.
- Consolini, G., M. F. Marcucci, M. Candidi, Multifractal structure of auroral electrojet index data, *Phys. Rev. Lett.*, **76**, 4082–4085, 1996.
- Consolini, G., and P. De Michelis, Non-Gaussian distribution function of *AE*-index fluctuations: Evidence for time intermittency, *Geophys. Res. Lett.*, **25**, 4087–4090, 1998.
- Edwards, J. W., A. S. Sharma and M. I. Sitnov, Spatio-temporal structure of geomagnetic activity triggered by dynamic pressure pulses: mutual information functional analysis, *Bull. Amer. Phys. Soc.*, **27**, 156, 2001.
- Freeman, M. P., N. W. Watkins and D.J. Riley, Evidence for a solar wind origin of the power law burst lifetime distribution of the *AE* indices, *Geophys. Res. Lett.*, **27**, 1087–1090, 2000.
- Frisch U., *Turbulence. The legacy of A.N. Kolmogorov*, (Cambridge University Press, Cambridge, 1995).
- Hnat, B., S. C. Chapman, G. Rowlands, N. W. Watkins, M. P. Freeman, Scaling in solar wind epsilon and the *AE*, *AL* and *AU* indices as seen by WIND, *Geophys. Res. Lett.*, **29**(10), 10.1029/2002GL016054, 2002.
- Hnat, B., S. C. Chapman, G. Rowlands, N. W. Watkins, M. P. Freeman, Correction to “Scaling in solar wind epsilon and the *AE*, *AL* and *AU* indices as seen by WIND”, *Geophys. Res. Lett.*, **30**(10), 10.1029/2003GL017194, 2003a.
- Hnat, B., S. C. Chapman and G. Rowlands, Intermittency, scaling, and the Fokker-Planck approach to fluctuations

- of the solar wind bulk plasma parameters as seen by the WIND spacecraft, *Phys. Rev. E* **67**, 056404, 2003b.
- Katsev, S, and I. L'Heureux, Are Hurst exponents estimated from short and irregular time series meaningful?, *Computers and Geosciences*, in press, 2001.
- Kovács, P., V. Carbone, Z. Vörös, Wavelet-based filtering of intermittent events from geomagnetic time series, *Planetary and Space Science*, *49*, 1219-1231, 2001.
- Lepping, R. P., *et al.* The WIND magnetic field investigation, *Space Sci. Rev.*, *71*, 207, 1995.
- Lui, A. T. Y., *et al.*, Is the dynamic magnetosphere an avalanching system?, *Geophys. Res. Lett.*, *27*, 911-914, 2000.
- Mandelbrot, B. B., *Gaussian Self-Affinity and Fractals: Globality, The Earth, 1/f Noise and R/S*, (Springer-Verlag, Berlin, 2002).
- Mantegna, R. N., & H. E. Stanley, Scaling behavior in the dynamics of an economic index, *Nature*, *376*, 46, 1995.
- Ogilvie, K. W., *et al.*, SWE, a comprehensive plasma instrument for the wind spacecraft, *Space Sci. Rev.*, *71*, 55-77, 1995.
- Rodríguez-Iturbe, I., & A. Rinaldo *Fractal River Basins: Chance and Self-Organization*, (Cambridge University Press, Cambridge, 1997).
- Sitnov, M. I., *et al.*, Phase transition-like behavior of the magnetosphere during substorms, *J. Geophys. Res.*, *105*, 12955-12974, 2000.
- Takalo, J., J. Timonen., and H. Koskinen, Correlation dimension and affinity of *AE* data and bicolored noise, *Geophys. Res. Lett.*, *20*, 1527-1530, 1993.
- Takalo J., and J. Timonen, Comparison of the dynamics of the *AU* and *PC* indices, *Geophys. Res. Lett.*, *25*, 2101-2104, 1998.
- Tsurutani, B. T., *et al.*, The nonlinear response of *AE* to the IMF B_s driver: A spectral break at 5 hours, *Geophys. Res. Lett.*, *17*, 279-282, 1990.
- Ukhorskiy, A. Y. , M. I. Sitnov, A. S. Sharma, K. Papadopoulos, On the origin of the power-law spectra in magnetospheric dynamics during substorms, *J. Geophys. Res.*, submitted, 2002.
- Uritsky, V. M., A. J. Klimas and D. Vassiliadis, Comparative study of dynamical critical scaling in the auroral electrojet index versus solar wind fluctuations, *Geophys. Res. Lett.*, *28*, 3809-3812, 2001.
- Vörös, Z., P. Kovács, Á. Juhász, A. Körmendi and A. W. Green, Scaling laws from geomagnetic time series, *Geophys. Res. Lett.*, *25*, 2621-2624, 1998.
- Watkins, N. W., M. P. Freeman, C. S. Rhodes, G. Rowlands, Ambiguities in determination of self-affinity in the *AE*-index time series, *Fractals*, *9*, 471-479, 2001.
-

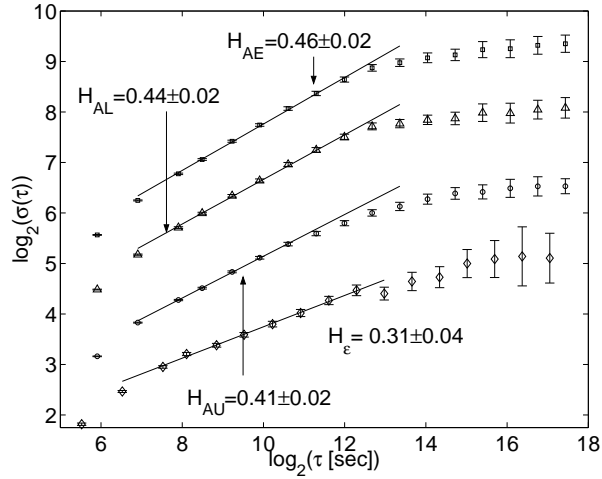


Figure 1. Scaling of the standard deviation of the PDFs of: \diamond - ϵ , \circ - AU index, \triangle - AL index and \square -the AE index. The plots have been offset vertically for clarity. Error bars are estimated assuming Gaussian statistics for the binned data.

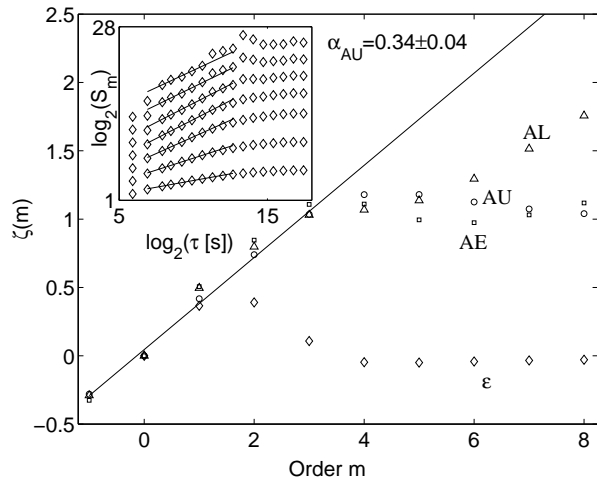


Figure 2. Dependence of the scaling exponent $\zeta(m)$ of the raw GSF on moment order m . Inset shows the GSF S_m versus time lag τ for AU .

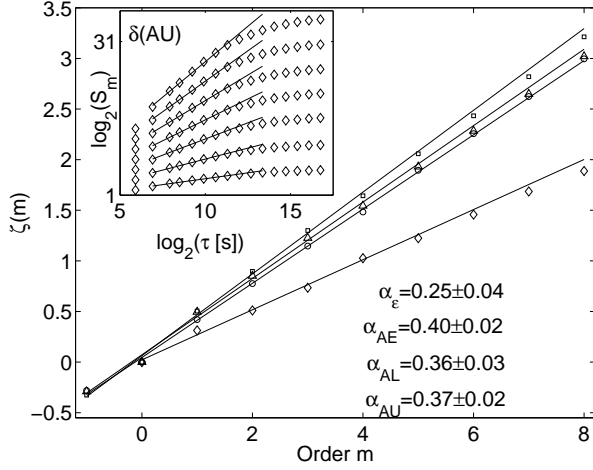


Figure 3. Dependence of the scaling exponent of the conditioned GSF on moment order. Inset shows the conditioned GSF S_m^c versus time lag τ for AU .

Quantity	α from $P(0, \tau)$	α from $\sigma(\tau)$	α from GSF	τ_{max} [min]
ϵ	-----	0.31 ± 0.04	0.25 ± 0.04	~ 100
AE	-0.47 ± 0.03	0.46 ± 0.02	0.40 ± 0.02	~ 100
AU	-0.46 ± 0.03	0.41 ± 0.02	0.37 ± 0.02	~ 60
AL	-0.45 ± 0.03	0.44 ± 0.02	0.36 ± 0.03	~ 100

Table 1. Scaling indices derived from $P(0, \tau)$, $\sigma(\tau)$ and GSF power laws.

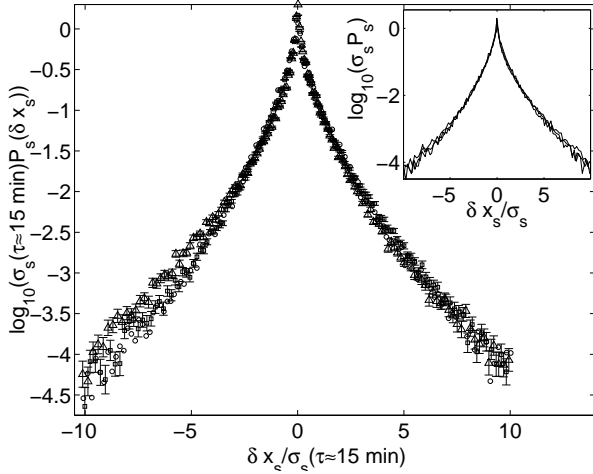


Figure 4. Direct comparison between the fluctuation PDFs for AE (\square), AU (\circ) and AL (\triangle), again at $\tau = 15$ minutes. Inset shows overlaid PDFs of AU , AE and $-AL$ fluctuations. Error bars as in Figure 1.

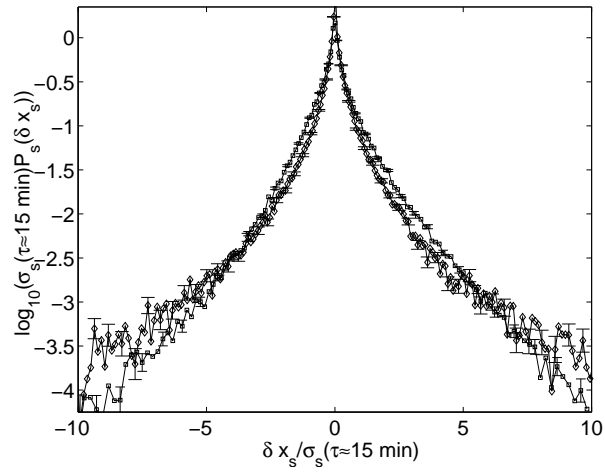


Figure 5. Direct comparison, for the particular choice $\tau = 15$ minutes, of the fluctuation PDFs for ϵ (\diamond) and AE index (\square). Error bars as in Figure 1.